ChemSusChem

Research Article
doi.org/10.1002/cssc.202301502

Chemistry Europe
European Chemical Societies Publishing

www.chemsuschem.org

Smart pillar[5]arene-based PDMAEMA/PES beads for selective dye pollutants removal: design, synthesis, chemical-physical characterization, and adsorption kinetic studies

Giulia Rando,[a, b] Silvia Sfameni,[b] Marco Milone,[a] Alessio Mezzi,[c] Marco Brucale,[d] Anna Notti,*[a] and Maria Rosaria Plutino*[b]

This article reports on the synthesis of an innovative smart polymer, P5-QPDMAEMA, opportunely developed with the aim of combining the responsiveness of PDMAEMA polymer and the host-guest properties of covalently linked pillar[5]arenes. Thanks to a traditional Non-Induced Phase Separation (NIPS) process performed at various coagulation pH, the blending of P5-QPDMAEMA with polyethersulfone gave rise to the formation of functional beads for the removal of organic dyes in water. Adsorption tests are carried out on all the produced blend-based beads by employing two representative dyes, the cationic methylene blue (MB), and the anionic methyl orange (MO). In particular, the P5-QPDMAEMA based beads, prepared at acidic pH, featured the best MO removal rate (i.e., 91.3% after 150 minutes starting from a 20 $mg \cdot L^{-1}$ solution) and a high selectivity towards the removal of the selected anionic dye. Based on the adsorption kinetics and isotherm calculations, the pseudo-first order and Freundlich models were shown to be the most suitable to describe the MO adsorption behavior, achieving a maximum adsorption capacity of 21.54 $mg \cdot g^{-1}$. Furthermore, zwitterionic beads are obtained by a post-functionalization of the PDMAEMA and the P5-QPDMAEMA based beads, to test their removal capability towards both anionic and cationic dyes, as shown.

1. Introduction

Nowadays, clean water is considered critical for human health and well-being, for nature and environment safeguard, as well as to ensure a regular social-economic growth. In particular, with the increase of the world population growth, and of the corresponding impacting anthropological activities (with related water needs from several industrial sectors), together with climate change effects, there is a great demand of accessing to safe and clean water. In this regard, since nowadays worldwide water sources are very vulnerable to environmental pollution, the development of efficient infrastructures for (waste)water management and treatment to protect and remediate suitable clean/drinking water sources is getting progressively more crucial. Unfortunately, until now conventional methods of (waste)water treatment still lack in the removal of the so-called "emerging contaminants" (such as organic dyes) that are nowadays widely used in textiles, leather, paper, plastic and cosmetic industries.[1,2] As a matter of fact, they represent a worrying threat to the human health for their chemical persistence and toxicity; for this reason new advanced techniques for (waste)water remediation are currently under investigation and settlement.[3–5]

In this contest, thanks to its excellent mechanical properties, as well as thermal and chemical stability,[6] polyethersulfone (hereafter PES) is widely used as an embedding polymer for the fabrication of nano- and ultrafiltration membranes for water purification. Furthermore, the preparation of functional PES-based systems, by its blending with other polymers, cross-linkers or nanofillers, leads to an improvement of its hydrophilicity, porosity, surface properties and adsorption performances.[7] For example, Amiri et al. developed a novel polyvinyl alcohol-graphene oxide-sodium alginate nanocomposite hydrogel blended PES nanofiltration membrane for improved water purification showing a Lanasol blue 3R dye rejection rate more than 83%.[8] In another study, Athira et al. focused on the efficient sulfonation of polyethersulfone polymer to generate sulfonated-polyethersulfone (SPES), as well as on the preparation of its blends with PES, to create cellulose

[a] G. Rando, M. Milone, A. Notti
Department of Chemical, Biological, Pharmaceutical and Environmental Sciences (ChiBioFarAm), University of Messina, Viale F. Stagno d'Alcontres 31, 98166, Messina, Italy
E-mail: anna.notti@unime.it

[b] G. Rando, S. Sfameni, M. R. Plutino
Institute for the Study of Nanostructured Materials, ISMN – CNR, URT Messina, c/o Dep. ChiBioFarAm, University of Messina, Viale F. Stagno d'Alcontres 31, 98166 Messina, Italy
E-mail: mariarosaria.plutino@cnr.it

[c] A. Mezzi
Institute for the Study of Nanostructured Materials, ISMN – CNR, via Salaria Km 29.3, 00015 Monterotondo stazione, Rome, Italy

[d] M. Brucale
Institute for the Study of Nanostructured Materials, ISMN – CNR, via P. Gobetti 101, 40129 Bologna, Italy

Supporting information for this article is available on the WWW under https://doi.org/10.1002/cssc.202301502

acetate CA/PES blend membranes and SPES/PES blend membranes, the latter characterized by a significantly lower hydrophobicity than the other developed membranes.[9]

PES-based beads may be also easily produced by simple and scalable approaches via the phase inversion method and so efficiently employed in filtrating systems. On this regard, some porous MOF@PES composite beads were developed by Valizadeh et al. and tested in a proof-of-concept device demonstrating an efficient capture and recovery capacity of more than 99% of I_2 from the feed solution, with the capability to be recycled and reused for multiple times.[10] Moreover, Zhang et al. prepared carboxyl-functionalized PES beads by in situ cross-linking polymerization and phase inversion methods, also featuring good reusability and storage stability for the safe and effective removal of urea.[11]

The adsorbent agents employed for the functionalization of PES-based blends and beads showed a significant impact on the selectivity/anti-interference ability, sensitivity, and extraction/desorption dynamics; the obtained results emphasize the importance of developing selective adsorption systems.

Stimuli-responsive polymers, a class of useful smart materials capable of adapting/reacting to the surrounding environment, may be also employed as efficient embedding systems. In particular, poly[2-(dimethylamino)ethylmethacrylate] (hereafter PDMAEMA) is a polymer sensitive to external stimuli such as temperature, pH and ionic strength, with already well-known applications ranging from therapeutic/biomedical fields to nanotechnology.[12]

Through various functionalization approaches, it is possible to implement PDMAEMA in order to show quite interesting and useful properties. Alotaibi et al. synthesized magnetic mesoporous silica nanoparticles modified with PDMAEMA brushes (Fe_3O_4@MSN-PDMAEMA), using surface-initiated Activators Regenerated by Electron Transfer (ARGET) atom transfer radical polymerization (ATRP). Tertiary amines in the polymer chains were quaternized using 2-iodoethanol to obtain cationic polymer chains with a permanent positive charge (Fe_3O_4@MSN-QPDMAEMA). The applicability of the synthesized materials in the removal of methyl orange (MO), and sunset yellow (E110) dyes from an aqueous solution was investigated. The experimental results proved that the Fe_3O_4@MSN-PDMAEMA sample exhibited a weaker adsorption performance toward both dyes, compared with Fe_3O_4@MSN-QPDMAEMA at a pH level above 5.[13]

Just recently, there has been a lot of interest in the development of new efficient adsorbent systems exploiting supramolecular approaches for the removal of target contaminants from various matrices.[14] On this regard, synthetic macrocycles, such as crown ethers, cyclodextrins, calixarenes, cucurbiturils and pillararenes, are characterized by large recognition cavities, thus playing an important role in host-guest chemistry.[14] In particular, pillar[5]arenes are a class of cyclooligomers consisting of 1,4-dimethoxybenzene units connected by methylene bridges in 2 and 5 position,[15,16] bearing an hydrophobic and electron-rich cavity (with a diameter of approximately 5 Å), and various phenolic oxygens suitable for functionalization. Thanks to these properties, pillar[5]arene derivatives have already shown to be able to effectively include several neutral and/or positively charged molecules (linear hydrocarbons, halogenalkanes, nitriles, amines, viologens) stabilized by multiple CH-π interactions or charge transfer complexes.[17] As a matter of fact, this class of macrocycles are already finding interesting applications in the sensing,[18,19] drug-delivery,[20] and catalysis[21] fields; furthermore, thanks to their selectivity towards the inclusion of various molecules, new recent examples of their use in combination with polymers in the separation, filtration and adsorption sectors are reported.[22,23] Within this framework, some examples relative to the production and the application of different adsorbent materials, based on inorganic or polymeric supports that take advantage of host-guest complexation of pollutant dye molecules by macrocyclic compounds, are well described in literature. Some studies, concerning pillar[5]arenes-based adsorbent materials, include: i) a quaternary cationic pillar[5]arene-modified zeolite, with a MO removal efficiency of 84% starting from an initial concentration of 100 $mg \cdot L^{-1}$ after 12 hours;[24] ii) a pillar[5]arene-based 3D-network polymer that featured a 95.2% uptake in 30 minutes of a 0.100 mM MO solution;[25] iii) a stimuli-responsive supramolecular polymeric network based on a bis-pillar[5]arene, showing a 83.2% of MO uptake in 30 minutes.[26]

More recent experimental findings include a novel form of polymeric dye adsorbent developed by Zang *et al.*, obtained by cross-linking a bis-hydrazide functionalized pillar[5]arene with trimesoyl chloride, that exhibit excellent promise in the selective adsorption and separation of small cationic dyes, like methylene blue (MB) and neutral red. Kinetic experimental findings showed that the pseudo-second order model and Freundlich isotherm model adequately predict the adsorption behaviors of both dyes. Moreover, this developed pillararene-based polymer adsorbent can be recycled five times with nearly little loss in adsorption performance.[27]

In this study, with the aim of combining the above-mentioned responsiveness of PDMAEMA polymer and the host-guest properties of the covalently linked pillararenes, the synthesis and characterization of a smart designed polymer (P5-QPDMAEMA), as obtained through the quaternarization of PDMAEMA with a pillar[5]arene derivative, was successfully carried out and reported.

Furthermore, PES/P5-QPDMAEMA blended polymers were prepared and used for the development of functional beads by a traditional Non-solvent Induced Phase Separation (hereafter NIPS) process carried out at various coagulation pH.

All the obtained final functional beads were investigated by ATR-FTIR, XPS, SEM and AFM techniques, in order to correlate their polymeric structures and reactivity; moreover, the adsorption performances for the removal of MB and MO, as representative cationic and anionic dye, respectively, were evaluated in water.

Adsorption kinetics and isotherm calculations were run on the beads featuring the best removal performances. Finally, by a post-functionalization of PDMAEMA and P5-QPDMAEMA beads, zwitterionic beads were produced and the adsorption

behaviour towards the removal of both the afore-mentioned cationic and anionic dyes is also reported.

2. Results and Discussion

2.1. Synthetic approaches towards P5-QPDMAEMA and NMR characterization

The designed smart polymer, P5-QPDMAEMA combining the responsiveness of PDMAEMA polymer (Figure 1a) and the host-guest properties of the covalently linked pillararenes (Figure 1b), was synthetized starting from a pillar[5]arene derivative (P5-Br) and PDMAEMA, both obtained according to literature procedures. In particular, the P5-Br derivative was synthetized by the co-pillarization of 1,4-dimethoxybenzene and 1-(2-bromoethoxy)-4-methoxybenzene according to the procedure described by Y. Zhou et al.,[28] meanwhile the PDMAEMA polymer by ARGET-ATRP of 2-(dimethylamino)ethyl methacrylate (DMAEMA)[29] using a monomer/catalyst/ligand/reducing agent molar ratios according to the method described by Willott et al.[30] and using the catalyst/initiator molar ratio suggested by Keating et al.[31] The final step towards the obtainment of the P5-QPDMAEMA polymer was a quaternarization process, involving the alkylation of the amino groups of PDMAEMA, by using the P5-Br derivative as alkylating agent (Figure 1c).

For these purposes a molar ratio of amino groups/P5-Br equal to 2:1 was used, where moles of amino groups mean the moles of dimethylaminoethyl groups present in the amount of PDMAEMA undergoing the alkylation reaction and they are calculated by dividing the weight of the polymer by that of the monomeric unit. ^{1}H and Diffusion Ordered Spectroscopy (DOSY) NMR experiments were performed on the final obtained polymer in order to assign, study and characterize its chemical structure. In Figure S1a the characteristic aromatic proton signals related to the pillararenic units,[16] as well as the aliphatic proton signals of PDMAEMA,[32] are evident. The DOSY plot in Figure S1b shows that pillararene and PDMAEMA signals have the same diffusion coefficient ($D_{obs} = 3.52\times10^{-11}$ m$^2\cdot$s^{-1}), thus confirming the covalent functionalization of the polymer. Careful integration of the aromatic resonances and of the PDMAEMA backbone methyl groups (resonances a in Figure S1a) showed that about one every five monomeric units in the polymer were alkylated by P5-Br.

2.2. Functional blend beads preparation

In order to produce easy to use adsorbent systems for the removal of target molecules from water,[33] we thought it worthwhile to prepare different types of beads based on blend polymers by a traditional NIPS process. In particular, four types of beads were prepared by solubilizing polyethersulfone (PES), polyvinylpyrrolidone (PVP, acting as pore former), and PDMAEMA or P5-QPDMAEMA, in dimethylacetamide (DMAc) as solvent; after 24 h the reaction mixture was dropped by the use of a syringe in three different coagulation baths (at different pH) to exploit the pH-responsiveness of PDMAEMA polymer (Figure 2).

All the produced beads, including the pristine ones (as the reference), are reported with the adopted name in Table 1, together with their composition.

The coagulation baths consisted in a 0.5 M solution of HCl, H_2O, and a 0.5 M solution of NaOH, labelled as a, n and b, respectively. The beads have been left in the baths for 2 h, and subsequently removed and left for 12 h in H_2O to fully coagulate.

Moreover, by post-functionalization[34] of the B-P(b) and B-P5QP(b), using 1,4-butansultone in methanol, two types of zwitterionic beads were produced and respectively indicated as B-P(zw) and B-P5QP(zw) (Figure 3). The functionalization percentage calculated through the eq. 1 in Experimental Section corresponds to 27.2% and 21.1%, respectively.

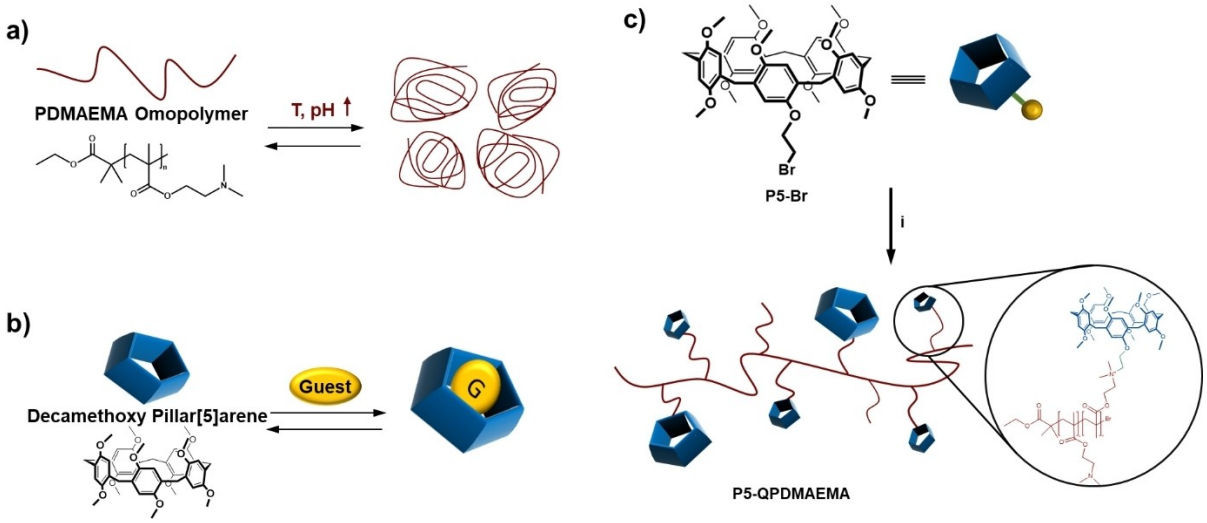

Figure 1. Graphical representation scheme of a) the stimuli-responsive properties of PDMAEMA polymer towards Temperature and pH variations, b) the host-guest properties of pillar[5]arenes towards a generic guest molecule and c) the synthesis of P5-QPDMAEMA (i. PDMAEMA, DMF, 323.15 K, 10 d).

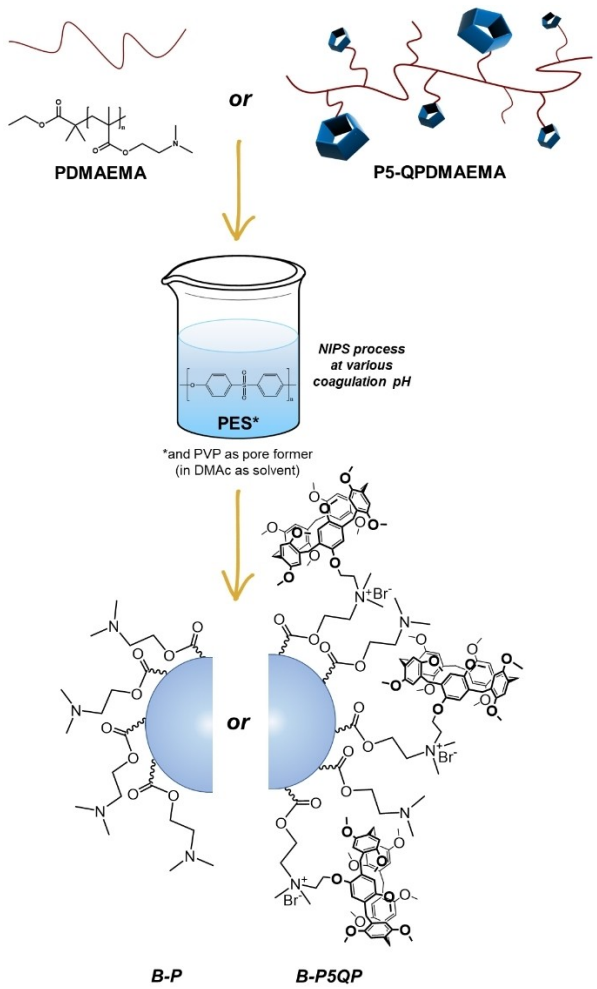

Figure 2. Graphical illustration of the production of the B-P and B-P5QP functional beads.

2.3. Chemical-physical, morphological and structural characterizations of the functional beads

2.3.1. ATR-FTIR spectroscopy

Attenuated total reflection infrared spectroscopy (ATR-FTIR) was used to determine the chemical composition of all the obtained beads systems, confirming their effective functionalization with the employed polymers. In Figure 4a the ATR-FT-IR spectra of the beads are represented, as prepared in neutral coagulation baths. A broad band can be observed at ~3300 cm^{-1} in all reported ATR-FTIR spectra due to the presence of some residual water. All the IR spectra display the typical signals of PES[35] like those at 3095 cm^{-1} and 3067 cm^{-1}, related to the presence of aromatic C–H groups.[36] After the addition of PVP, signals at 2955 cm^{-1} relative to C–H alkyl groups and at 1656 cm^{-1} of the C=O amido groups appears. The presence of PDMAEMA in the B-P beads was confirmed by the characteristic signals of the polymer[37,38] at 2773 cm^{-1} and 2827 cm^{-1}, corresponding to C–H and $-N(CH_3)_2$ groups, and also the peak at 1725 cm^{-1}, corresponding to the C=O ester group. Finally, in the B-P5QP beads a new signal at 1038 cm^{-1} appears, attributed to O–C groups of the pillararene units.[39]

The comparison of ATR-FTIR spectra in Figure 4b of B-P(b), B-P (zw), B-P5QP(b) and B-P5QP(zw) shows new signals in the zwitterionic beads at 1350 cm^{-1}, 909 cm^{-1} and 781 cm^{-1}, respectively, assigned to the S=O, S–O and C–S groups inserted after the post-functionalization reaction.

2.3.2. SEM microscopy

In order to evaluate their bulk morphology, beads were dissected with a sharp scalpel, metallized with Au and imaged via Scanning Electron Microscopy (SEM). The observed structures (see Figure 5) are compatible with those usually observed in other analogous PES-based systems prepared via the NIPS process.[33]

The pore diameter of the obtained PES-based beads are clearly affected by the composition of the starting polymeric blend.[40] As the pores are generated during the phase-separation process, the solubility of the different polymers in the solvent DMAc is the major responsible of the pore formation; PVP shows high solubility in coagulation bath (deionized water) while PES is insoluble. A fast exchange process of the solvent (DMAc), additive (PVP) and coagulation bath takes place resulting in a different porosity (more numerous and smaller pores) of the beads.[41] Subsequently, the different solubility of PDMAEMA and P5-QPDMAEMA affects the cross-section morphology of the corresponding B-P and B-P5QP resulting beads. While all beads display generally porous structures, those prepared in basic coagulation baths are characterized by a slightly lower structural homogeneity than the ones prepared at acidic pH, as well as a smaller average pore size due to the pore-forming effect of the employed

Table 1. Ratio[a] of the reagents employed to produce the beads.

Name	PES [%]	PVP [%]	PDMAEMA [%]	P5-QPDMAEMA [%]	DMAc [%]
Pristine	20	–	–	–	80
B[b]	18	2	–	–	80
B-P[c]	18	1	1	–	80
B-P5QP[d]	18	1	–	1	80

a) Ratio w/w %; b) B=Blend, i.e., blend polymer based on PES and PVP; c) B-P, i.e. blend polymer based on PES, PVP and PDMAEMA; d) B-P5QP, i.e. blend polymer based on PES, PVP and P5-QPDMAEMA.

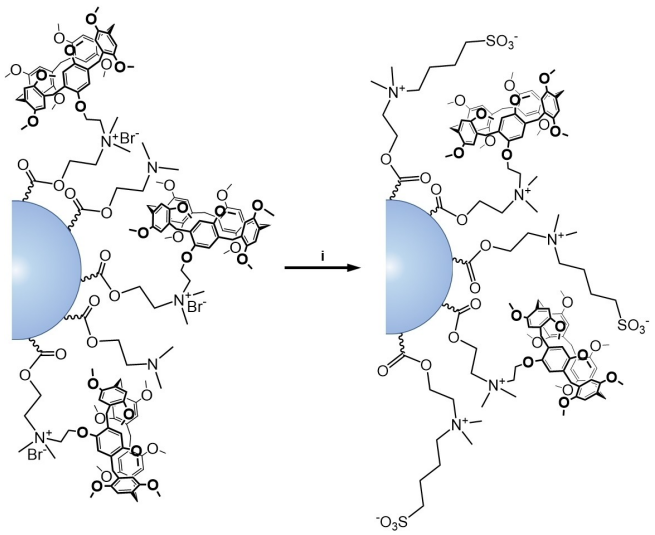

Figure 3. Graphic synthetic scheme of the formation of B-P5QP(zw) zwitterionic bead (i. 1,4-butansultone, CH_3OH, 313.15 K, 24 h).

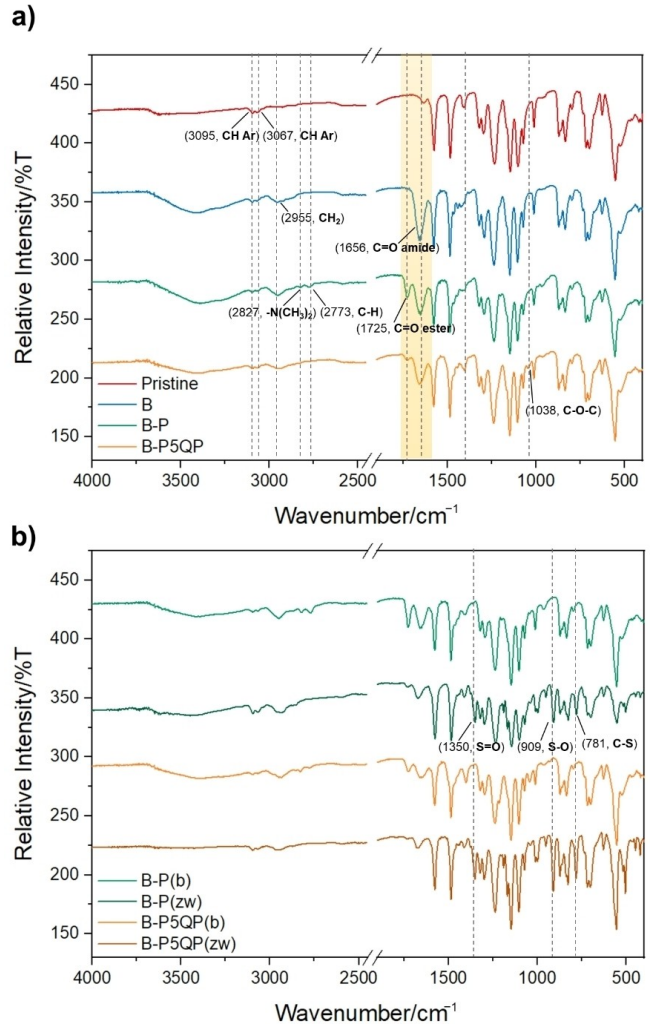

Figure 4. ATR-FTIR spectra of beads prepared in a) neutral coagulation bath, and b) basic coagulation bath, before and after the post-functionalization with 1,4-butansultone.

polymers at such pH value.[42] In contrast, the cross section structure of P5-QPDMAEMA-based beads is characterized by smaller pores showing a more homogeneous distribution regardless of the pH. This can be attributed to different factors: (i) viscosity of the starting polymeric blend,[43] (ii) potential presence of less PDMAEMA pH-sensitive amino groups, due to their partial substitution with pillararenic units, which results in a lesser degree of morphological variation. The structure of B-P5QP(zw) was also characterized by SEM analysis, evidencing no significant morphological variations induced by the post-functionalization process.

2.3.3. XPS spectroscopy

X-Ray photoelectron measurement is a very surface sensitive analysis able to provide information on the oxidation state of the detected elements. All investigated samples were characterized by the presence of C, O, S and N. Depending on the pH, the presence of Na and Cl, in their typical oxidation state Na^+ (BE(Na1s) = 1071.5 eV) and Cl^- (BE(Cl2p) = 199.5 eV) was alternatively detected. Figure 6a shows the comparison of C1s spectra acquired on the pristine samples at different pH. The peak fitting analysis evidenced that the signals were characterized by three peaks, positioned at BE = 285.0 eV, 286.5 eV and 292.0 eV and assigned to C–C, C–O and π-π^* shake-up satellite, respectively.

This last contribution is typical of the aromatic structure, which is found in the PES compound.[44] Upon pH variation, the shape of the C1 signals was substantially the same except for the appearance of the –COOH(R) contribution (BE = 290.0 eV) at basic pH values. The sulfonyl functional groups were identified by the presence of the S2p signal, characterized by its typical doublet $S2p_{3/2}$-$S2p_{1/2}$ separated in energy by 1.2 eV, where the $S2p_{3/2}$ peak was positioned at BE = 168.0 eV. Operating at basic pH values, a second peak assigned to a sulphonate group appeared at BE = 168.7 eV. Beads prepared by the combination of PES and PVP, evidenced the same structure of the C 1s signal with a further component positioned at BE = 287.6 eV, characteristic for the C=O (Figure 6b) and, at the same time, a single N 1s peak positioned at BE = 399.7 eV due to the amidic group. The functionalization of the beads with PDMAEMA and P5-QPDMAEMA induced the separation of the N 1s components positioned at BE = 399.7 ÷ 399.8 eV and 402.0 ÷ 402.8 eV, assigned to amine and ammonium groups, respectively (Figure 6c).

2.4. Qualitative MB and MO adsorption tests

To understand the relevance of the functionalization of the beads as innovative systems with implemented characteristics than common PES based solutions in the separation of emerging contaminants from water, some preliminary batch tests were carried out (Figure 7).

Qualitative preliminary adsorption tests on all the produced systems were performed by immersion of a single bead (3 mg)

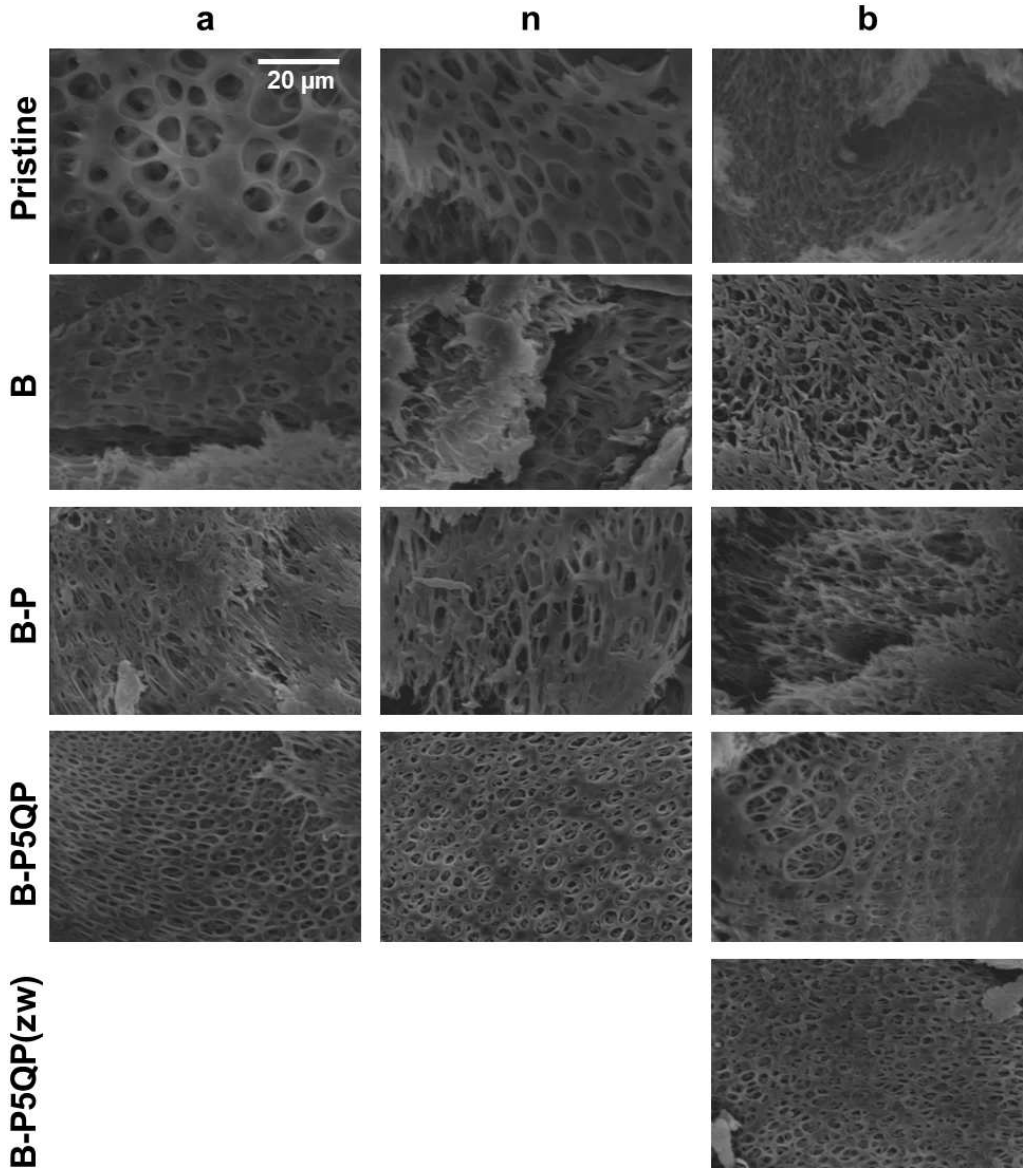

Figure 5. SEM images of the cross-sections of Pristine, B, B-P, B-P5QP and B-P5QP(zw) beads prepared at acidic (left column), neutral (central column) or basic pH (right column). All images are taken at the same magnification. The scale bar in the top left panel applies to the whole set.

in 2 mL of 100 μM water solution of each selected dye. In particular, MB was selected as representative cationic dye, and MO as anionic dye.

After 24 h at room temperature each bead was removed from the respective solution, washed with distilled water, and dried on filter paper. In Figure 7a, the Pristine and B beads show qualitatively the best adsorption performances towards the removal of MB, while B-P and B-P5QP beads show the best removal efficiency for MO.

To highlight the selectivity of the beads, the same adsorption test was performed by using an equimolar solution of MB and MO ([MB] = [MO] = 50 μM, V_{tot} = 2 mL). As shown in Figure 7b, after 24 h the Pristine and B beads appeared with a dark green colour, indicating the non-selective adsorption of both dyes. The green colouring fades in the B-P beads and it almost totally disappears in the B-P5QP ones, thus indicating a minor efficacy in removing MB for the electrostatic repulsion effect between the cationic charged PDMAEMA and P5-QPDMAEMA polymers and methylene blue dye.[45]

In particular, the B-P5QP beads prepared in acidic coagulation bath, showed the best selectivity towards the removal of the anionic dye MO, probably because of the presence of more protonated amino groups in the PDMAEMA chains and the possible host-guest interactions between the pillararenic units and the dye. The reason for these observed differences is most likely related to the surface charge of each bead, varying from the negatively charged surface of the Pristine and B beads (i.e. due to the sulfonic acid groups of PES),[46] until the positively charged one of the B-P and B-P5QP beads, due to the partial or total protonation/quaternarization of the amino groups present in the PDMAEMA chains.

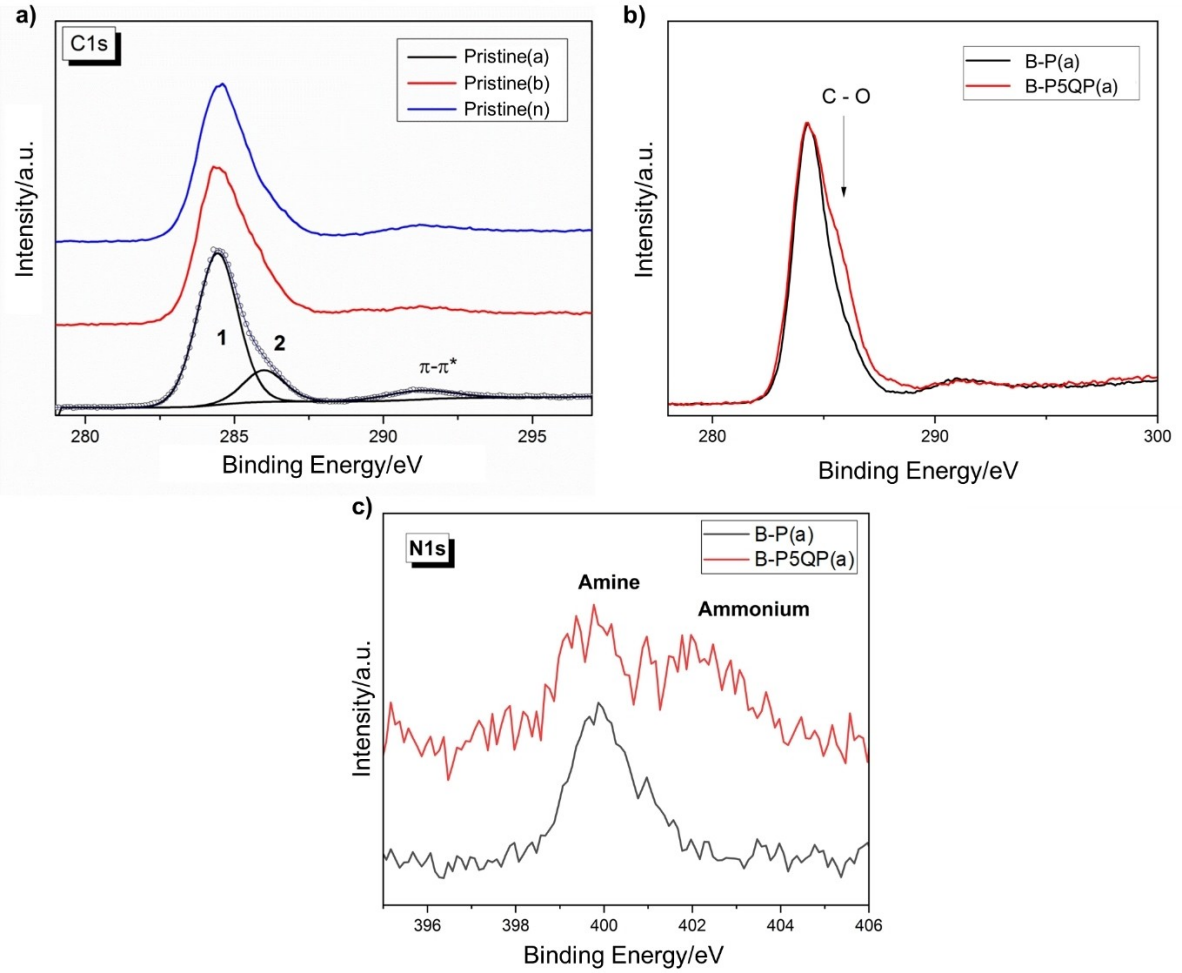

Figure 6. Comparison of: a) C 1s signal acquired on the pristine samples and the peaks assigned to C–C (1) and C–O (2) bonds; b) C 1s signal and c) N 1s signal of B-P(a) and B-P5QP(a) beads.

Finally, adsorption test, performed with B-P5QP(zw) beads, showed the capability of this zwitterionic systems towards the retention of both anionic and cationic dyes (Figure 7c).

2.5. Beads adsorption performances

2.5.1. Performances comparison

In order to confirm the affinity of the PDMAEMA-based beads (B-P and B-P5QP) towards the anionic MO dye, the removal percentage (%) and adsorption capacity (q_t/mg·g^{-1}) of the functional beads were determined according to the equation n. 2 and 3 (see Experimental Section). To this end, a comparison of the performances between different beads was carried out (Figure 8). In particular, each type of functional bead (≈60 mg) was immersed in 10 mL of a 20 mg·L^{-1} MO solution for 150 minutes.

Under these experimental conditions, the B-P5QP(a) beads showed the highest removal rate (91.3 %) and adsorption capacity (3.06 mg·g^{-1}) achieving the quasi-total discoloration of the solution.

2.5.2. Effect of the initial MO concentration

With the aim of evaluating the mass transfer resistance from the solution to the solid phase that may affects the adsorption of the dye, the effect of the initial MO concentration on a fixed quantity of B-P5QP(a) beads was investigated (Figure 9a,b) by immersing ≈20 mg of B-P5QP(a) beads in 10 mL MO solutions at different concentrations (i.e. 10, 20, 40, 80, 150 and 300 mg·L^{-1}).

From the experimental results reported in Figure 9a,b, it is evident how the removal percentage becomes lower, in both cases, at higher MO concentration, most probably due to the saturation of the active sites of the functional beads. Furthermore, in the experiment run over 24 hours, there is a minimum in the observed adsorption capacity at [MO] = 80 mg·L^{-1} (plot b). As previously reported for similar systems,[47] this behaviour could be ascribed to an equilibrium between the MO/bead adducts and the free MO molecules in solution, taking place due to the beads surface saturation, which locally increases the inter-beads ionic strength. Reversely, an adsorption capacity of 14.91 mg·g^{-1} was achieved after 5 h of contact time of a 300 mg·L^{-1} MO solution (plot a).

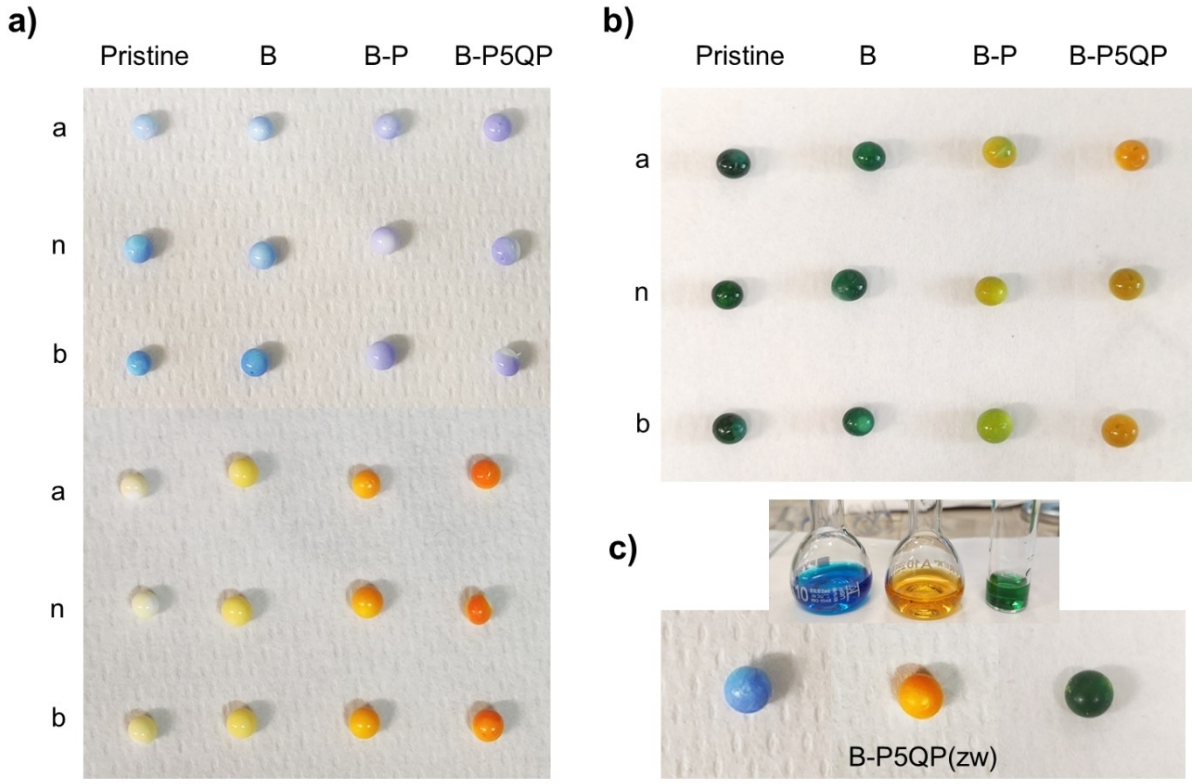

Figure 7. Qualitative beads adsorption test results of: a) MB or MO, where each row (from top to bottom) represents a bead produced at an acidic (a), neutral (n) or basic (b) coagulation bath; b) both MB and MO ([MB] = [MO] = 50 μM, V_{tot} = 2 mL); c) MB, or MO, or mixed solution of both dyes (from left to right) by the zwitterionic bead B-P5QP(zw).

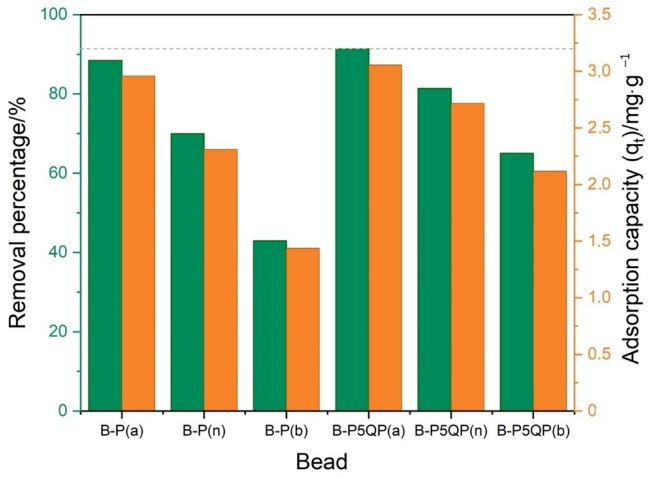

Figure 8. Histogram plot relative to the comparison of the removal percentage and adsorption capacity of different functional beads after a contact time of 150 minutes in a 20 mg·L^{-1} MO solution.

2.5.3. Effect of adsorbents concentrations

To understand the adsorption behaviour of B-P5QP(a) beads and the mechanism of their interaction with MO, the effect of adsorbent concentration was studied. Different amounts of B-P5QP(a) beads (≈3, 10, 20, 35, 60 mg) were poured in 10 mL of a 20 mg·L^{-1} MO solution and left react for 120 minutes (Figure 9c).

The experiment showed that the dye removal percentage increases with the increase of the bead quantity (green points), but adsorption capacity shows its maximum at lower beads weights (see Figure 9c). When the bead quantity is considerably low, the adsorption active sites can rapidly combine with adsorbates until saturation by dye molecules; meanwhile, at higher beads quantity (i.e., > 3 mg), even if there are more overall active sites to be potentially involved in the adsorption process, still the more exposed and available surface area to MO molecules is not linearly dependent from the final bead quantity. In fact, as the amounts of adsorbents increase (i.e. bead quantity), the beads assume a stack modular configuration, thus reducing and modifying their whole specific exposed surface area. As a consequence, a concentration gradient between the solution and the beads internal surface seems to be promoted and the diffusion resistance correspondently increases.[48] This phenomenon could be an explanation of the lack of trend for the observed adsorption capacities.

2.5.4. Contact time effect

The effect of the contact time between ≈20 mg of B-P5QP(a) beads and 20 mL of a 20 mg·L^{-1} MO solution was studied, as reported in Figure 9d. As showed in the graph both the removal percentage and the corresponding adsorption capacity increase with the adsorption time increase. After a contact time of

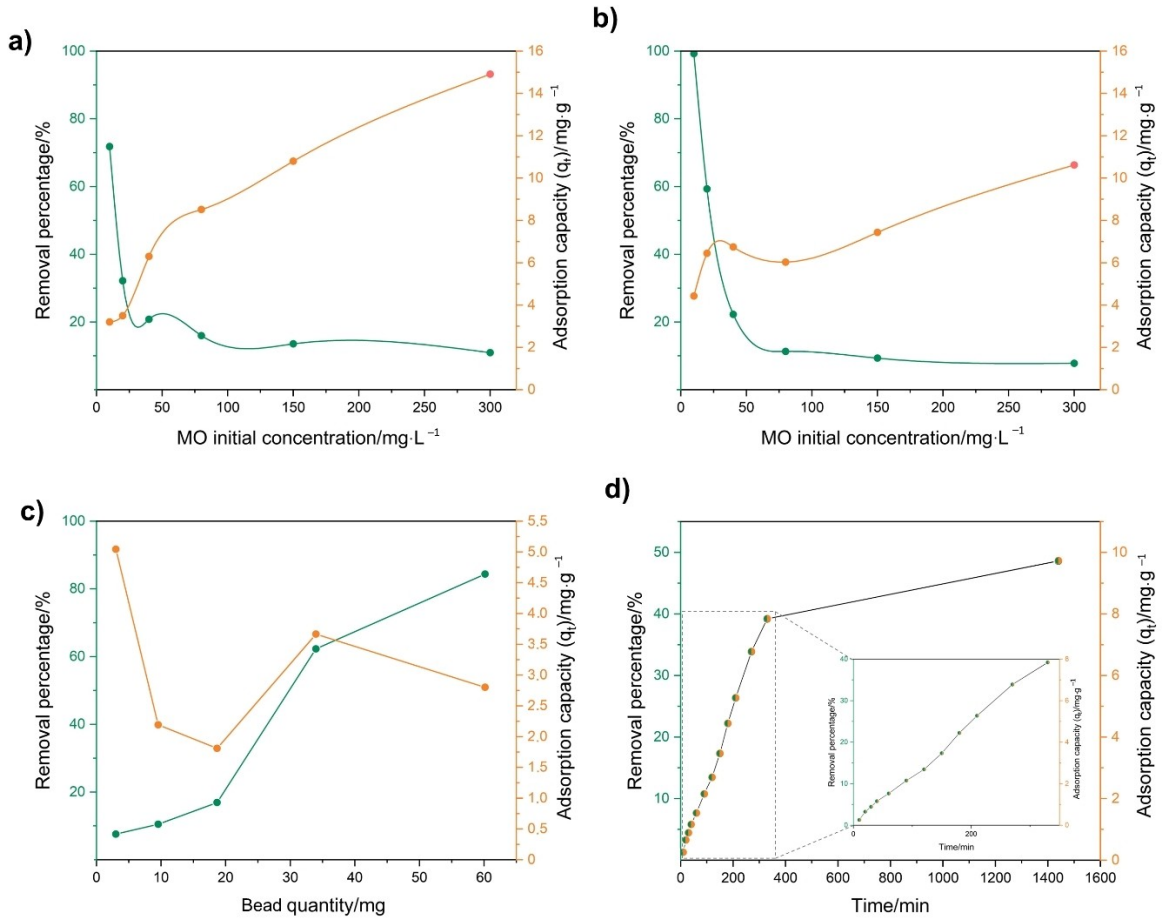

Figure 9. Plots showing the removal percentage (left vertical axis) and adsorption capacity (right vertical axis) of B-P5QP(a) beads a-b) *versus* different MO concentrations after 5 h and 24 h of contact time, respectively; c) as a function of B-P5QP(a) beads amount into a 20 mg·L^{-1} MO solution and after a contact time of 120 minutes; d) as a function of time for B-P5QP(a) beads immersed into a 20 mg·L^{-1} MO solution.

330 min, the 39% of MO removal with a 7.8 mg·g^{-1} of adsorption capacity was reached. The internal diffusion resistance can lead to an initial lower adsorption capacity (or either removal percentage), as shown by the sigmoidal shape of the first data point trend (see inset in figure 9d) that also indicates an induction time for the adsorption/removal process. After 24 h the 46.6% of MO removal with a 9.7 mg·g^{-1} was achieved as the adsorption capacity equilibrium value.

2.5.5. Adsorption kinetics

A kinetic study has been performed to evaluate the adsorption mechanism towards the removal of MO from the B-P5QP(a) bead. On this regard, four different non-linear kinetic models (pseudo-first order, pseudo-second order, intraparticle diffusion, Elovich models) were employed (Figure 10, Table 2). The equations and methods used are showed in the experimental section.

Pseudo-first and pseudo-second order models are widely used for the study of the adsorption behaviour of solid/liquid systems.[49] Moreover, the intra particle diffusion model has been also widely used for the evaluation of the rate-limiting step of adsorption kinetics, by studying the process that can involve the mass transfer of adsorbate (film diffusion), and

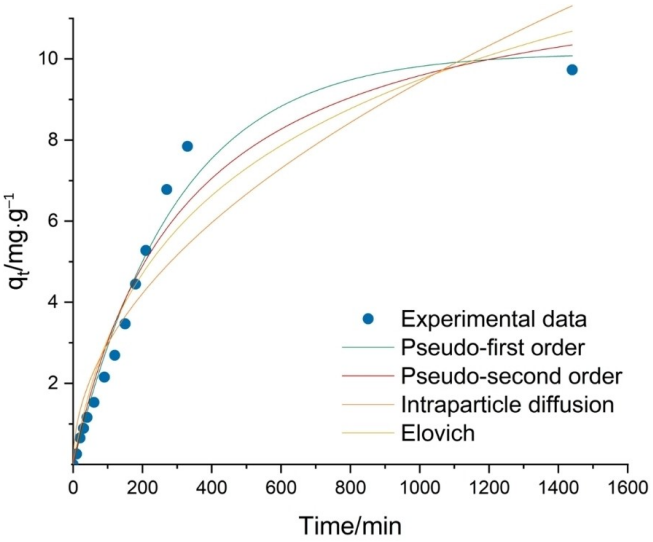

Figure 10. Plot of the adsorption capacity of MO by B-P5QP(a) beads as a function of time together with kinetic models fitting.

Table 2. Adsorption kinetic rate constants for different applied mechanism models for the adsorption of MO by B-P5QP(a) beads.

Pseudo-first order				Pseudo-second order		
$q_{e,exp}$/mg·g^{-1}	q_e/mg·g^{-1}	k_1/min^{-1}	R^2	q_e/mg·g^{-}	k_2/g mg^{-1}·min^{-1}	R^2
9.73	10.16	0.0034	0.9762	12.61	2.52	0.9582
Intraparticle diffusion				Elovich		
$q_{e,exp}$/mg·g^{-1}	kdiff/mg·g−1 ·min−0.5		R2	α/mg·g−1·min−	β/g·mg−1	R2
9.73	0.2982		0.8645	0.05	0.2881	0.9334

surface diffusion.[50] The most recent kinetic model employed for this type of adsorption studies is the Elovich one, developed by Zeldowitsch to understand the chemisorption nature of adsorption by the determination of the mass diffusion, surface diffusion, activation, and deactivation energy.[51]

On the light of the calculations, the correlation coefficient R^2 of the pseudo-first order model (0.9762) is the higher one. The degree of closeness between the theoretical and experimental adsorption capacities can also be used as a basis for the determination of the goodness of fit of different kinetic models. Additionally, the pseudo-second order model has also a good correlation factor, thus meaning that this reaction model is significant in the rate-controlling step, and therefore, the physisorption or chemisorption adsorption processes may be indistinguishable in certain situations and can occur simultaneously.[52]

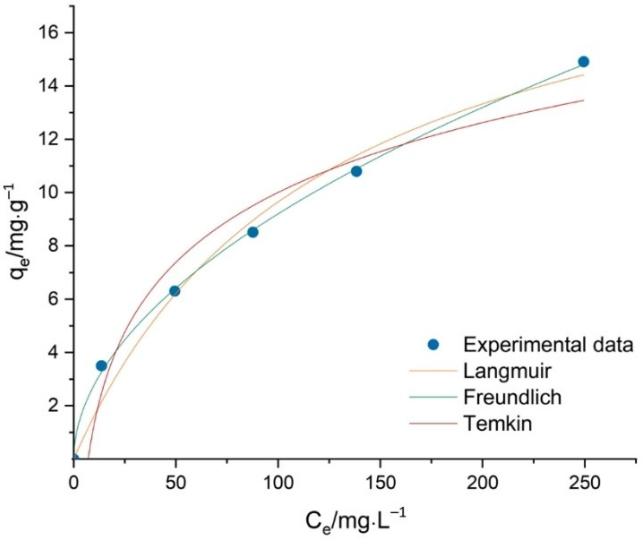

Figure 11. Plot showing the B-P5QP(a) bead adsorption capacities as a function ofdifferent MO equilibrium concentrations together with isotherm models fitting.

2.5.6. Adsorption isotherms

In order to understand the adsorbent − adsorbate interactions and the design of the adsorption system B-P5QP(a), three adsorption isotherm models were evaluated by means of the most common Langmuir and Freundlich models, and also the Temkin model (Figure 11, Table 3).

On this regard, the Langmuir isotherm model describes the equilibrium between adsorbate and adsorbent system, where the dye molecules will form a monolayer onto the sorption sites; on the other hand, the Freundlich isotherm model assumes that multilayer adsorption occurs on the surface of the adsorbent characterized by a heterogeneous surface.[53] Moreover, Temkin isotherm model that undertakes the heat of sorption is linear rather than logarithmic, was also evaluated.[54]

The Freundlich equation fits better the experimental adsorption data with an R^2 of 0.9988. In particular, in agreement with previous studies, this model usually may predict an increase of the adsorbed dye concentrations on the adsorbent system with increase of the added dye concentration in the solution,[55] while the adsorption energy exponentially decreases with the saturation of the reactive sorption centres,[56] in accordance with the obtained experimental data. This model also referred to heterogeneous surfaces, as mentioned above, and therefore it is also applicable to systems in which is involved a monolayer (like chemisorption) and multilayer adsorption processes (like Van der Waals adsorption).[50] Moreover, 1/n (where n is the Freundlich isotherm constant, see eq. 9 in the Experimental Section) represents a heterogeneity factor and it indicates a chemisorption process for 1/n value between 0.1 and 1, while a physisorption process for $1/n > 1$.[57] It is well known that the adsorption behaviour between an adsorbent and an adsorbate may occur through different mechanisms as the formation of chemical bonds, ion exchange, electrostatic interactions, van der Waals forces hydrophobic attraction, hydrogen bonding, and physical adsorption.[58] In this studied case, the B-P5QP(a) bead can exploit different of these mechanisms, as also possible due to host-guest interactions

Table 3. Isotherm equilibrium constants for different applied fitting models relative to the adsorption of MO by B-P5QP(a) beads.

Langmuir			Freundlich			Temkin		
q_m/mg·g^{-1}	k_L/L·mg^{-1}	R^2	1/n	k_F /L·g^{-1}	R^2	B_T	k_T/L·mg^{-1}	R^2
21.541	0.00812	0.9812	0.5199	0.8396	0.9988	3.780	0.141	0.9614

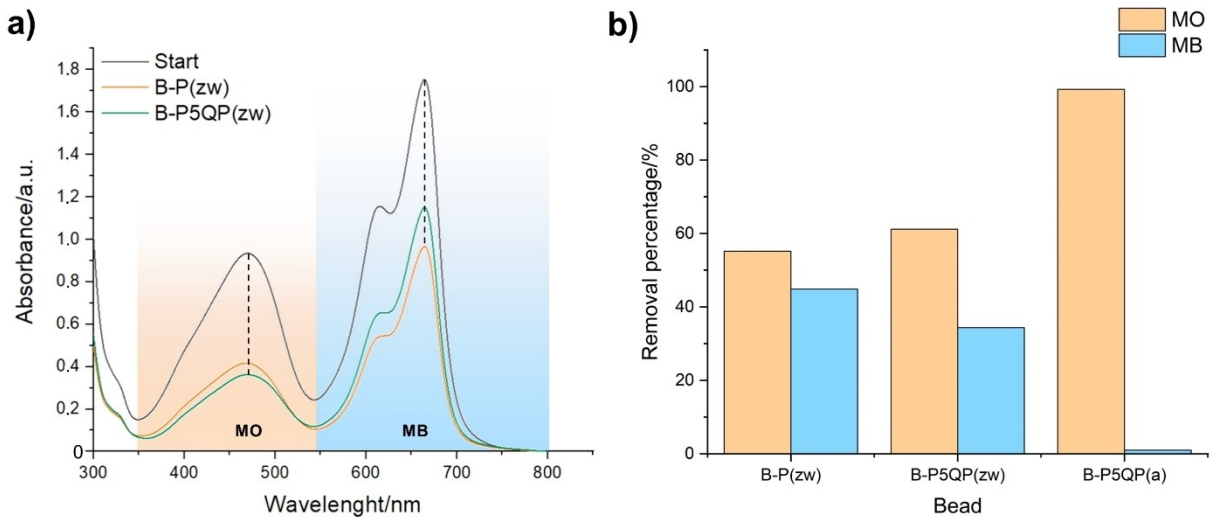

Figure 12. a) Adsorption spectra of MB + MO solution treated by each zwitterionic bead (≈20 mg) after a contact time of 24 h; b) removal percentage of both dyes by each type of zwitterionic beads and B-P5QP(a) bead.

between pillararenic units and dye molecules. Therefore, it is possible to describe the adsorbent – adsorbate interactions between MO dye and B-P5QP(a) beads as a multilayer physio/chemisorption heterogeneous process, in agreement with the Freundlich isotherm model.

2.6. Zwitterionic beads adsorption performances

The B-P(zw) and B-P5QP(zw) beads were tested for the removal of both MB and MO dyes.

A mixed solution based on MB 20 $mg \cdot L^{-1}$ (5 mL) and MO 20 $mg \cdot L^{-1}$ (5 mL) was employed to study the adsorption properties of the zwitterionic beads (Figure 12).

Both zwitterionic beads showed the capability to remove the tested anionic and cationic dyes from the solution. In particular, B-P(zw) beads showed the best adsorption performance towards MB with a removal percentage of 44.9%, instead B-P5QP(zw) beads featured the higher MO uptake with a removal percentage of 61.1%.

The dye adsorption behaviour of B-P(zw) bead can be ascribed to the presence of less permanent cationic functionalities for the absence of the P5-Br units linked to the amino groups of PDMAEMA, but also of an increased number of negative charged sites due to the higher degree of functionalization with 1,4-butansultone compared to B-P5QP(zw) bead. On the other hand, the good adsorption of B-P5QP(zw) beads towards both dyes may be ascribed to a combined effect of more available cationic charged sites[45,59] together with the host-guest interactions between the MO/MB molecules and the pillararenic units.[24,37]

The proposed adsorption behaviour, depicted in Figure 13, showing weak electrostatic and host-guest interactions taking place between MO/MB and quaternary nitrogen, sulfonato groups and pillararene cavity, may explain how quaternary

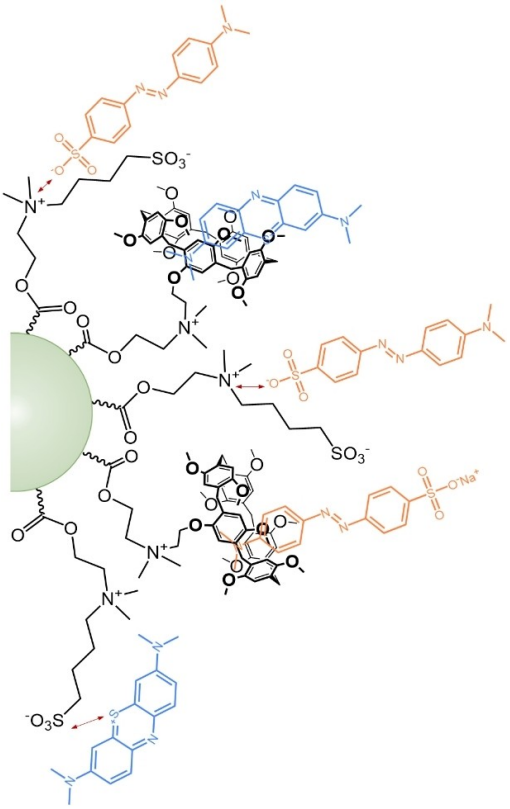

Figure 13. Illustration of the proposed behaviour of B-P5QP(zw) bead for the removal of both MB and MO dyes.

post-functionalization makes easier the simultaneous removal of both the cationic and anionic dyes.

A comparison of the removal percentage of MO anionic and MB cationic dyes by B-P5QP(a), B-P(zw), and B-P5QP(zw) zwitterionic beads with other already developed beads is given in Table 4.

Table 4. MO and MB removal percentage comparison of different developed bead adsorbent systems at pH = 7 and T~25 °C.

PES-based system	Total Volume/ mL	Starting MO conc./ $mg \cdot mL^{-1}$	Starting MB conc./ $mg \cdot mL^{-1}$	MO removal/ %	MB removal/ %	Ref.
CG/PGMA*	25	–	50	–	76.0–89.9	[60]
CMC/dextran sulfate/diatomite*	50	50	–	62–98	–	[61]
Alg-Xan-CPC**	2.5	20	20	86.1	47.5	[62]
Hectorite clay-alginate**	50	25	25	22	100	[63]
MNPs-PES*	5	10	10	38.56	72.94	[64]
B-P5QP(a)**	10	10	10	99.27	< 2	This work
B-P(zw)**	10	10	10	55.17	44.86	This work
B-P5QP(zw)**	10	10	10	61.14	34.38	This work

*data obtained from two independent MO or MB removal experiments. ** data obtained from simultaneous MB and MO removal experiments

The first two systems reported in Table 4 were tested with MO or MB, while all the others are systems comparable with the PES-based beads obtained and studied in this work. B-P5QP(a) beads definitely show the best selectivity towards MO, while other hectorite clay-alginate[63] beads have instead the best selectivity towards MB. First of all, it must be considered that in the textile industry anionic or direct dyes (i.e., anionic dye in the form of salts) are much more common and used than cationic ones; the former are used for dyeing wool and other protein fibres, polyamides, cotton, linen, viscose, while the cationic ones are used only for colouring acrylic fibres.[65–67] Furthermore, unlike all other reported systems, B-P5QP(a) beads have the very important characteristic of being able to be implemented with a zwitterionic functionality; although B-P(zw) and B-P5QP(zw) beads present a lower, but still satisfactory, percentage of removal of both dyes, they turn out to be potentially antifouling.

As a matter of fact, all the obtained materials, as described in the previous paragraphs, may contribute to the development of innovative and smart membranes useful for water filtration approaches. Moreover, the post-functionalization method leads not only to a different adsorption behaviour compared to the starting beads, but could be useful also for the preparation of zwitterionic membranes[68] with potential antifouling performances. In this regard, we must mention that fouling, brought on by substances found in wastewater, such as inorganic substances, bacteria, proteins, and other organic molecules[69] to mention some, is still one of the main issues with membrane technology. This occurring problem reduces the membranes efficiency and lifespan, thus leading to increased energy consumption since higher working pressures are required and, therefore, economical significant losses can occur. Following already published studies on zwitterionic antifouling coatings or treatments on membranes,[70,71] the antifouling performances of B-P(zw) and B-P5QP(zw) developed systems are currently in progress.

3. Conclusions

A smart hybrid polymer P5-QPDMAEMA, based on a pillar[5]arene and the stimuli-responsive polymer PDMAEMA, was successfully obtained and employed for the preparation of functional blended polymeric beads, containing either PES and PVP. All beads, as obtained by NIPS process at various coagulation pH, were first qualitatively tested for the removal of MB and MO from water; all experimental findings showed that the P5-QPDMAEMA based beads featured the best removal performances and the higher selectivity towards the MO anionic dye. A removal percentage and an adsorption capacity of 91.3% and 3.06 $mg \cdot g^{-1}$, respectively, were achieved in an experiment carried out on the B-P5QP(a) beads (≈60 mg) added to a MO solution (V = 10 mL, [MO] = 20 $mg \cdot L^{-1}$) after 150-minute reaction time, as clear by the almost total discoloration of the solution. The effect of MO concentration, quantity of adsorbent and contact time of B-P5QP(a) beads were evaluated and the experimental results show that an adsorption capacity of 14.91 $mg \cdot g^{-1}$ was achieved after 5 h of contact time of a 300 $mg \cdot L^{-1}$ MO solution.

Adsorption kinetics and isotherm calculations resulted more in accordance with the pseudo-first order and Freundlich models that best define the MO adsorption behaviour of B-P5QP(a) bead with a q_m of 21.54 $mg \cdot g^{-1}$. Its adsorption performance can be described through a physio/chemisorption process involving a multilayer heterogeneous surface. Furthermore, the obtained B-P(zw) and B-P5QP(zw) zwitterionic beads showed a relevant removal capability of both tested anionic and cationic dyes. As a matter of fact, those systems can represent a valuable advanced and innovative approach for the selective removal of organic dyes from contaminated water; additionally, these polymeric blends can be employed for the preparation of functional and smart membranes for textile wastewater treatment approaches with improved antifouling performances for the zwitterionic B-P(zw) and B-P5QP(zw) systems.

Experimental section

Materials and methods

All employed chemical reagents, i.e. 1,4-dimethoxy benzene, parafolmaldehyde, ethyl α-bromoisobutyrate (EBiB), N, N, N′, N′′, N′′-pentamethyldiethylenetriamine (PMDETA), ascorbic acid, hydrochloric acid, sodium hydroxide, magnesium sulphate, polyethersulfone (PES), polyvinylpyrrolidone (PVP), methyl orange, methylene blue, the solvents methanol, dimethylformamide (DMF), dichloromethane, hexane, N,N-dimethylacetamide (DMAc) and deuterated solvent $CDCl_3$, were commercially available at most purity grade available from Sigma Aldrich and used as received. The monomer 2-(dimethylamino)ethyl methacrylate (DMAEMA) was purchased from Sigma Aldrich and passed through a basic alumina column to remove the hydroquinone monomethyl ether inhibitor. Where possible the synthesis reactions were monitored by thin layer chromatography on silica gel plates with fluorescence indicator, displaying chromophores by UV ($\lambda = 254$ nm), or by treatment with acid dodeca-phosphomolybdic in ethanolic solution (5% w/v). Column chromatography for the purification of the synthetic products was performed using 230–400 mesh silica gel as the stationary phase.

^{1}H NMR spectra were acquired at a temperature of 298 K using a Varian 500 MHz spectrometer. The chemical shifts (δ) are reported in ppm with respect to the residual protiated signal of the solvent, while the values of the coupling constants (J) are reported in Hz.

Fourier transform infrared analysis (ATR-FTIR) were acquired directly on a whole bead by using a V-6600 Jasco Spectrometer (JASCO Europe s.r.l., Cremella, LC, Italy), equipped with an attenuated Total Reflection accessory, including the Spectra Manager™ Suite with integrated search software solution, KnowItAll® Informatics and database JASCO Edition (JASCO Europe s.r.l., Cremella, LC, Italy). Spectra were recorded at room temperature, in the range of 4000–500 cm^{-1} acquiring 32 scans per data set with a resolution of 4 cm^{-1}.

UV-Vis spectroscopy measurements were performed with a Jasco V-770 UV-Vis spectrophotometer (JASCO Europe s.r.l., Cremella, LC, Italy) equipped with standard measurement and analysis programs and the Spectra Manager™ Suite Spectroscopy Software (JASCO Europe s.r.l., Cremella, Italy), at ~25 °C.

SEM micrographs were acquired on a Hitachi S4000 SEM operated at 15 kV. Beads were carefully sliced with a sharp scalpel to expose their bulk material. Thin slices were mounted onto an aluminum stub (PELCO) and metallized with a ≈10 nm-thick 99.999% Au (Sigma-Aldrich) layer by means of a sputter coater (Quorum QR150R).

X-ray Photoelectron Spectroscopy (XPS) measurements, were performed using an ESCALAB 250Xi (Thermo Fisher Scientific Ltd., East Grinstead, UK) spectrometer, equipped with a monochromatized Al kα source (hυ = 1486.6 eV) and 6-channeltron as detection system. The experiments were carried out with the constant pass energy set to 40 eV. During the measurements, the charge neutralization of the insulator samples, was guaranteed by an electron flood gun, operating at large spot area compensation mode. All spectra were registered and processed with Thermo Avatange software v5.979 (Thermo Fisher Scientific Ltd., East Grinstead, UK).

Synthetic procedures

Synthesis of P5-Br

The pillar[5]arene derivative was synthesized according to a literature procedure.[28]

A mixture of 1,4-dimethoxy benzene (1.67 g, 12.1 mmol), paraformaldehyde (0.44 g, 14.6 mmol), 1-(2-bromoethoxy)-4-methoxy benzene (0.7 g, 3.0 mmol) and $[BF_3 \cdot O(C_2H_5)_2]$ (1.9 mL, 15.3 mmol) in 1,2-dichloroethane anhydrous (50 mL), was kept under stirring in an inert atmosphere (Ar). After 3.5 h at room temperature, the reaction was stopped by adding a mixture of distilled water and methanol 2:1 v/v (150 mL) and keep stirring for 2 h. The mixture was filtered on a sintered glass filter and the solvent evaporated. The dried solid in the flask was solubilized in CH_2Cl_2 (100 mL), washed with distilled H_2O (2×50 mL), dried with $MgSO_4$ and finally the solvent was evaporated. The reaction crude was purified by column chromatography (eluent mixture 1:3 hexane/CH_2Cl_2), obtaining P5-Br as a white crystalline solid (1.25 g, 1.48 mmol, 50%).

^{1}H NMR (500 MHz, $CDCl_3$): δ 6.80–6.76 (m, 9H, ArH), 6.70 (s, 1H, ArH), 4.04 (t, $J = 6.0$ Hz, 2H, OCH_2), 3.81–3.77 (m, 10H, $ArCH_2Ar$), 3.68–3.64 (m, 27H, CH_3), 3.44 (t, $J = 6.0$ Hz, 2H, $BrCH_2$) ppm.

Synthesis of PDMAEMA

Poly[2-(dimethylamino)ethyl methacrylate] (PDMAEMA) was synthesized by an ARGET-ATRP according to methods described by Willott et al.[30] and Keating et al.[31]

$CuBr_2$ (2.65 mg, 0.012 mmol), DMAEMA (5 mL, 30 mmol), PMDETA (25 μL, 0.12 mmol), EBiB (17 μL, 0.023 g, 0.12 mmol) and ascorbic acid (20.90 mg, 0.12 mmol were added in chronological order to a degassed solution of methanol/H_2O (v/v = 9:1). The final ratio DMAEMA/$CuBr_2$/PMDETA /Ascorbic acid/EBiB is 2500:1:10:10:10 and DMAEMA/solvent ratio 1:1 v/v. The reaction was allowed to continue for 20 h in a thermostated bath at 35 °C under inert atmosphere (Ar). The reaction mixture was poured in H_2O at boiling temperature (150 mL), the precipitate recovered and dried under vacuum at 40 °C for 2 h. The solid product was dissolved in HCl (200 mL, 1 M) and precipitated with NaOH (150 mL, 2 M). The obtained precipitate was recovered and dissolved in CH_2Cl_2 (100 mL), the organic phase was washed with distilled water (3×20 mL), dried with $MgSO_4$ and finally the solvent was evaporated. The obtained polymer was dissolved in CH_2Cl_2 (100 mL) and precipitated by adding hexane (80 mL). After eliminating the solvent, the polymer was washed with hexane and dried under vacuum at 40 °C for 2 h obtaining a transparent rubbery solid (3 g), stored at 4 °C.

^{1}H NMR (500 MHz, $CDCl_3$): δ 4.09 (br, 2H, $CH_2OC{=}O$), 2.62 (br, 2H, NCH_2), 2.32 (s, 6H, $N(CH_3)_2$), 1.84 (br, 2H, CH_2), 1.26 (s, CCH_3), 1.05–0.91 (br, 3H, CH_3) ppm.

Synthesis of P5-QPDMAEMA

PDMAEMA (100 mg) and P5-Br (257 mg, 0.3 mmol) were poured in DMF (5 mL) and keep reacting under stirring at 50 °C for 10 days. Subsequently CH_2Cl_2 (2 mL) and hexane (4 mL) were added to the reaction mixture and keep stirring until the formation of a precipitate. The product was separated from the solvent and dried under vacuum obtaining a transparent glassy like product (243 mg).

^{1}H NMR (500 MHz, $CDCl_3$): δ 6.84–6.51 (m, 10H, ArH), 4.06 (br, 2H, $CH_2OC{=}O$), 4.06 (br, 2H, OCH_2), 3.75 (br, 10H, $ArCH_2Ar$), 3.63–3.49

(br, 27H, CH_3), 3.38 (br, 2H, $BrCH_2$), 2.58 (br, 2H, NCH_2), 2.28 (s, 6H, $N(CH_3)_2$), 1.88 (br, 2H, CH_2), 1.24 (s, CCH_3), 1.04–0.87 (br, 3H, CH_3) ppm.

Preparation of PES beads

Polyethersulfone blends were prepared by mixing selected polymers with the ratio (w/w) indicated in Table 1, in DMAc as solvent and keep stirring for 12 h at room temperature. Before the production of the beads, the casting solutions were placed in ultrasound bath for 30 minutes to remove bubbles.

The beads were prepared thanks to a traditional Non-solvent Induced Phase Separation (NIPS) process performed at various coagulation pH, using a 1 cc syringe (G26, 0.45 mm×12 mm) and a 1.20×40 mm (18G ×1$^1/_2$") needle, placing it at a distance of 5 cm from the coagulation bath. The injection speed was controlled at 50–70 drops per minute. Three coagulation baths were used: i) HCl (50 mL, 0.5 M), ii) H_2O (50 mL), NaOH (50 mL, 0.5 M). Beads were left for 2 h in the coagulation baths and subsequently removed and left for 12 h in a H_2O bath (100 mL). After the coagulation beads (~2 mm of diameter) were abundantly washed with H_2O and ethanol and dried at 50 °C for 24 h.

Zwitterionic beads preparation

The post functionalization of B-P(b) and B-P5QP(b) beads was performed by the immersion of ≈145 mg of each kind of bead in 8 mL of MeOH with 0.8 g of 1,4-butansultone and keeping stirring at 40 °C for 24 h. The beads were subsequently washed with distilled water and ethanol and dried at 50 °C until constant weight. The functionalization percentage was calculated gravimetrically with the Eq. 1:[72]

$$\textit{Functionalization percentage}\ \% = \frac{W_f - W_i}{W_i} \times 100 \quad (1)$$

where W_f/mg and W_i/mg are the final and the initial weight, respectively.

Adsorption tests

Calibration curves and adsorption measurements of MB and MO were obtained using a UV-Vis V-770, Jasco spectrophotometer at ~25 °C. The concentration of MB was determined at λ/nm = 664, and MO at λ/nm = 464.

Removal efficiencies (%) of MB and MO by the different beads were calculated by the formula:

$$\% = \frac{(C_0 - C_t)}{C_0} \times 100\,\% \quad (2)$$

where C_0/mg·L^{-1} and C_t/mg·L^{-1} are the dye concentrations at initial time and time t.

Adsorption capacity (q_t/mg·g^{-1}) was determined according to the formula:

$$q_t = \frac{(C_0 - C_t)V}{W} \quad (3)$$

where C_0/mg·L^{-1} and C_t/mg·L^{-1} are the dye concentrations at initial time and time t; V/L is the solution volume and W/g is the adsorbent mass.

In Figure 9 interpolate lines between experimental data points are qualitative and shown only to better visualize the process trend.

Kinetic study

B-P5QP(a) beads (≈20 mg) and 20 mg·L^{-1} MO solution (20 mL) were employed for the kinetic study after drying until constant weight. After each time interval the absorbance measured with the UV–Vis spectrophotometer at λ/nm = 464, ~25 °C.

All the parameters were calculated from the graph of the adsorption capacity at time t (q_t/mg·g^{-1}) vs t/min.

Coefficients of regression (R^2) of all the different types of models have been evaluated and assessed to determine the best fit of the appropriate model.

For the pseudo-first order calculation the following equation was employed:[49,73]

$$q_t = q_e(1 - e^{-k_1 t}) \quad (4)$$

where t/min is the contact time, q_t/mg·g^{-1} is the adsorption capacity at time t, q_e/mg·g^{-1} the adsorption at equilibrium, k_1/min^{-1} is the adsorption rate constants of pseudo-first order adsorption model.

For the pseudo-second order calculation the following equation was employed:[49]

$$q_t = \frac{q_e^2 k_2 t}{1 + q_t k_2 t} \quad (5)$$

where t/min is the contact time, q_t/mg·g^{-1} is the adsorption capacity at time t, q_e/mg·g^{-1} the adsorption capacity at equilibrium, k_2/g·mg^{-1}·min^{-1} is the adsorption rate constants of pseudo-second order adsorption model.

For the intraparticle diffusion calculation the following equation was employed:[50,74]

$$q_t = k_{diff} t^{1/2} + C \quad (6)$$

where t/min is the contact time, q_t/mg·g^{-1} is the adsorption capacity at time t, k_{diff}/mg·g^{-1}·min$^{-0.5}$ is the adsorption rate constants of intraparticle diffusion adsorption model and C is a constant.

For the Elovic calculation the following equation was employed:[51,75]

$$q_t = \frac{1}{\beta}\ln(\alpha\beta t + 1) \quad (7)$$

where t/min is the contact time, q_t/mg g^{-1} is the adsorption capacity at time t, α/mg·g^{-1}·min^{-1} is the rate of adsorption, β/g·mg^{-1} is the desorption constant.

3.1. Adsorption isotherms

B-P5QP(a) beads (≈20 mg, dried until constant weight) and 20, 40, 80, 150 and 300 mg·L^{-1} MO solutions (10 mL) were employed for the adsorption isotherm study. After a contact time of 5 h the

absorbance measured with the UV–Vis spectrophotometer at λ/nm = 464 and a temperature of ~25 °C.

All the parameters were calculated from the graph of the adsorption capacity at the equilibrium (q_e/mg·g^{-1}) vs the equilibrium dye concentration C_e/mg·L^{-1}.

Coefficients of regression (R^2) of all the different types of models have been evaluated and assessed to determine the best fit of the appropriate model.

For the Langmuir calculation the following equation was employed:[53,76]

$$q_e = \frac{q_m k_L C_e}{1 + k_L C_e} \quad (8)$$

where C_e/mg·L^{-1} is the equilibrium dye concentration in the solution, k_L/L·mg^{-1} is the Langmuir adsorption constant, and q_m/mg·g^{-1} is the theoretical maximum adsorption capacity.

For the Freundlich calculation the following equation was employed:[53,77]

$$q_e = k_F C_e^{1/n} \quad (9)$$

where k_F/L·mg^{-1} and n represent the Freundlich isotherm constants indicating the capacity and intensity of the adsorption, respectively.

For the Temkin calculation the following equation was employed:[54,78]

$$q_e = B_T ln(k_T C_e) \quad (10)$$

Where B_T/J·mol^{-1} correspond to RT/b (T is the absolute temperature in K, R the universal gas constant) and k_T/L·mg^{-1} is the Temkin isotherm constant related to the heat of adsorption.

Acknowledgements

MUR and CNR are gratefully acknowledge for financial support. The authors acknowledge the financial support of the PON-MIUR "Ricerca e Innovazione 2014–2020" RESTART (design and development of smaRt advancEd materials and Sustainable Technologies for wAteR Treatment) PhD project and PRIN_20179BJNA2 grant. This work has been partially funded by European Union (NextGeneration EU), through the MUR-PNRR project SAMOTHRACE (SiciliAn MicronanOTecH Research And Innovation CEnter ECS00000022). All authors wish to thank S. Romeo, G. Napoli, G. Bellanti and F. Giordano for technical and informatic assistance in all instrumentation set-up and subsequent data fitting. The corresponding authors Anna Notti and Maria Rosaria Plutino contributed equally to the paper.

Conflict of Interests

The authors declare no conflict of interest.

Data Availability Statement

The data that support the findings of this study are available from the corresponding author upon reasonable request.

Keywords: Pillararenes · smart materials · PDMAEMA · polyethersulfone · organic dyes · water remediation · selective adsorbents

[1] A. Tkaczyk, K. Mitrowska, A. Posyniak, *Sci. Total Environ.* **2020**, *717*, 137222.
[2] G. Rando, S. Sfameni, M. R. Plutino, *Gels* **2023**, *9*, 9 DOI 10.3390/gels9010009.
[3] A. K. Badawi, M. Abd Elkodous, G. A. M. Ali, *RSC Adv.* **2021**, *11*, 36528.
[4] I. Ielo, F. Giacobello, S. Sfameni, G. Rando, M. Galletta, V. Trovato, G. Rosace, M. R. Plutino, *Materials (Basel).* **2021**, *14*, 1.
[5] G. Rando, S. Sfameni, M. Galletta, D. Drommi, S. Cappello, M. R. Plutino, *Mol.* **2022**, *27*, 4856 DOI 10.3390/molecules27154856.
[6] K. Wang, A. A. Abdalla, M. A. Khaleel, N. Hilal, M. K. Khraisheh, *Desalination* **2017**, *401*, 190.
[7] T. A. Otitoju, A. L. Ahmad, B. S. Ooi, *RSC Adv.* **2018**, *8*, 22710.
[8] S. Amiri, A. Asghari, V. Vatanpour, M. Rajabi, *Sep. Purif. Technol.* **2020**, *250*, 117216.
[9] V. B. Athira, S. Mohanty, S. K. Nayak, *Mater. Today Commun.* **2020**, *25*, 101544.
[10] B. Valizadeh, T. N. Nguyen, B. Smit, K. C. Stylianou, *Adv. Funct. Mater.* **2018**, *28*, 1801596.
[11] J. Zhang, Z. Wang, C. He, X. Liu, W. Zhao, S. Sun, C. Zhao, *ACS Omega* **2019**, *4*, 2853.
[12] M. Wei, Y. Gao, X. Li, M. J. Serpe, *Polym. Chem.* **2017**, *8*, 127.
[13] K. M. Alotaibi, A. A. Almethen, A. M. Beagan, H. M. Al-Swaidan, A. Ahmad, S. A. Bhawani, A. M. Alswieleh, *Appl. Sci.* **2021**, *11*, 10451 DOI 10.3390/app112110451.
[14] J. Ma, Y. Zhang, B. Zhao, Q. Jia, *Anal. Chim. Acta* **2020**, *1122*, 97.
[15] M. Xue, Y. Yang, X. Chi, Z. Zhang, F. Huang, *Acc. Chem. Res.* **2012**, *45*, 1294.
[16] T. Ogoshi, S. Kanai, S. Fujinami, T. Yamagishi, Y. Nakamoto, *J. Am. Chem. Soc.* **2008**, *130*, 5022.
[17] T. Ogoshi, M. Hashizume, T. Yamagishi, Y. Nakamoto, *Chem. Commun.* **2010**, *46*, 3708.
[18] T. Ogoshi, T. Yamagishi, *Eur. J. Org. Chem.* **2013**, *2013*, 2961.
[19] I. Pisagatti, D. Crisafulli, A. Pappalardo, G. Trusso Sfrazzetto, A. Notti, F. Nastasi, M. F. Parisi, N. Micali, G. Gattuso, V. Villari, *Mater. Today Chem.* **2022**, *24*, 100841.
[20] L. Barbera, D. Franco, L. M. De Plano, G. Gattuso, S. P. P. Guglielmino, G. Lentini, N. Manganaro, N. Marino, S. Pappalardo, M. F. Parisi, F. Puntoriero, I. Pisagatti, A. Notti, *Org. Biomol. Chem.* **2017**, *15*, 3192.
[21] K. Wang, J. H. Jordan, K. Velmurugan, X. Tian, M. Zuo, X.-Y. Hu, L. Wang, *Angew. Chem. Int. Ed.* **2021**, *60*, 9205.
[22] Z. Li, Y.-W. Yang, *Adv. Mater.* **2021**, *n/a*, 2107401.
[23] X. Ji, H. Wang, H. Wang, T. Zhao, Z. A. Page, N. M. Khashab, J. L. Sessler, *Angew. Chem. Int. Ed.* **2020**, *59*, 23402.
[24] Y. Yang, J. Yang, Y. Du, C. Li, K. Wei, J. Lu, W. Chen, L. Yang, *ACS Omega* **2019**, *4*, 17741.
[25] B. Shi, H. Guan, L. Shangguan, H. Wang, D. Xia, X. Kong, F. Huang, *J. Mater. Chem. A* **2017**, *5*, 24217.
[26] T.-B. Wei, L.-H. Qi, Q.-P. Zhang, W.-H. Zhang, H. Yao, Y.-M. Zhang, Q. Lin, *New J. Chem.* **2020**, *44*, 12531.
[27] G. Zhang, X.-Y. Lou, M.-H. Li, Y.-W. Yang, *Dyes Pigm.* **2022**, *206*, 110576.
[28] Y. Zhou, G. Zhang, B. Li, L. Wu, *ACS Appl. Mater. Interfaces* **2020**, *12*, 30761.
[29] H. Dong, K. Matyjaszewski, *Macromolecules* **2008**, *41*, 6868.
[30] J. D. Willott, B. A. Humphreys, T. J. Murdoch, S. Edmondson, G. B. Webber, E. J. Wanless, *Phys. Chem. Chem. Phys.* **2015**, *17*, 3880.
[31] J. J. Keating IV, A. Lee, G. Belfort, *Macromolecules* **2017**, *50*, 7930.
[32] Q. Zhao, P. Ni, *Polymer* **2005**, *46*, 3141.
[33] C.-C. Ho, J. F. Su, *Polymer* **2022**, *241*, 124560.
[34] L.-J. Zhu, L.-P. Zhu, Y.-F. Zhao, B.-K. Zhu, Y.-Y. Xu, *J. Mater. Chem. A* **2014**, *2*, 15566.
[35] Z. Geng, X. Wang, H. Jiang, L. Zhang, Z. Chen, Y. Feng, W. Geng, X. Yang, M. Huo, J. Sun, *Polym.* **2019**, *11*, 555 10.3390/polym11030555.

[36] M. A. Hossain, M. Elias, M. M. Rahman, M. M. Rahman, M. S. Ali, M. A. Razzak, *Bangladesh J. Sci. Ind. Res.* **2020**, *55*, 139.
[37] Y. Zhou, Y. Hu, W. Huang, G. Cheng, C. Cui, J. Lu, *Chem. Eng. J.* **2018**, *341*, 47.
[38] L.-P. Yang, P. Zou, C.-Y. Pan, *J. Mater. Chem.* **2009**, *19*, 1843.
[39] Y. Liu, B. Lou, L. Shangguan, J. Cai, H. Zhu, B. Shi, *Macromolecules* **2018**, *51*, 1351.
[40] X. Deng, T. Wang, F. Zhao, L. Li, C. Zhao, *J. Appl. Polym. Sci.* **2007**, *103*, 1085.
[41] L. Gzara, Z. A. Rehan, S. Simone, F. Galiano, N. T. Hassankiadeh, S. F. Al-Sharif, A. Figoli, E. Drioli, *Journal of Polymer Engineering* **2017**, *37*, 69.
[42] S. Zhao, Z. Wang, J. Wang, S. Wang, *J. Membr. Sci.* **2014**, *469*, 316.
[43] P. Amirabedi, R. Yegani, M. K. Razavi Aghje, *J. Text. Polym.* **2013**, *1*, 24.
[44] J. A. Gardella, S. A. Ferguson, R. L. Chin, *Appl. Spectrosc.* **1986**, *40*, 224.
[45] C. Li, H. Zhu, X. She, T. Wang, F. She, L. Kong, *RSC Adv.* **2016**, *6*, 67242.
[46] D. Breite, M. Went, I. Thomas, A. Prager, A. Schulze, *RSC Adv.* **2016**, *6*, 65383.
[47] J. Chen, F. Tendeyong, S. Yiacoumi, *Environ. Sci. Technol.* **1997**, *31*, 1433.
[48] X. Tao, Y. Wu, L. Cha, *Environ. Sci. Pollut. Res. Int.* **2019**, *26*, 19828.
[49] H. Moussout, H. Ahlafi, M. Aazza, H. Maghat, *Karbala Int. J. Mod. Sci.* **2018**, *4*, 244.
[50] E. E. Jasper, V. O. Ajibola, J. C. Onwuka, *Appl. Water Sci.* **2020**, *10*, 132.
[51] J. López-Luna, L. E. Ramírez-Montes, S. Martinez-Vargas, A. I. Martínez, O. F. Mijangos-Ricardez, M. del C. A. González-Chávez, R. Carrillo-González, F. A. Solís-Domínguez, M. del C. Cuevas-Díaz, V. Vázquez-Hipólito, *SN Appl. Sci.* **2019**, *1*, 950.
[52] S. J. Allen, Q. Gan, R. Matthews, P. A. Johnson, *J. Colloid Interface Sci.* **2005**, *286*, 101.
[53] K. L. Yu, X. J. Lee, H. C. Ong, W.-H. Chen, J.-S. Chang, C.-S. Lin, P. L. Show, T. C. Ling, *Environ. Pollut.* **2021**, *272*, 115986.
[54] C. A. Başar, *J. Hazard. Mater.* **2006**, *135*, 232.
[55] A. R. Nešić, S. J. Veličković, D. G. Antonović, *Composites Part B* **2013**, *53*, 145.
[56] G. Crini, *Dyes Pigm.* **2008**, *77*, 415.
[57] S. Pandey, N. Son, M. Kang, *Int. J. Biol. Macromol.* **2022**, *210*, 300.
[58] N. Hou, R. Wang, F. Wang, J. Bai, J. Zhou, L. Zhang, J. Hu, S. Liu, T. Jiao, *ACS Omega* **2020**, *5*, 5470.
[59] Q. Lin, K. Wang, M. Gao, Y. Bai, L. Chen, H. Ma, *J. Taiwan Inst. Chem. Eng.* **2017**, *76*, 65.
[60] S. Lapwanit, T. Sooksimuang, T. Trakulsujaritchok, *J. Environ. Chem. Eng.* **2018**, *6*, 6221.
[61] T. Benhalima, F. Z. Allali, N. Roumane, H. Ferfera-Harrar, *J. Mol. Liq.* **2023**, *383*, 122150.
[62] S. Biswas, A. Pal, *Mater. Today Commun.* **2022**, *33*, 104386.
[63] R. R. Pawar, Lalhmunsiama, P. Gupta, S. Y. Sawant, B. Shahmoradi, S.-M. Lee, *Int. J. Biol. Macromol.* **2018**, *114*, 1315.
[64] L. Y. Yee, Q. H. Ng, S. H. Shuit, S. K. Enche Ab Rahim, D. Mohammad Nawi, S. C. Low, *Environ. Prog. Sustain. Energy* **2021**, *40*, e13699.
[65] S. Samsami, M. Mohamadizaniani, M.-H. Sarrafzadeh, E. R. Rene, M. Firoozbahr, *Process Saf. Environ. Prot.* **2020**, *143*, 138.
[66] J. Sharma, S. Sharma, V. Soni, *Reg. Stud. Mar. Sci.* **2021**, *45*, 101802.
[67] H. B. Slama, A. Chenari Bouket, Z. Pourhassan, F. N. Alenezi, A. Silini, H. Cherif-Silini, T. Oszako, L. Luptakova, P. Golińska, L. Belbahri, *Appl. Sci.* **2021**, *11*, 6255 DOI 10.3390/app11146255.
[68] N. AlSawaftah, W. Abuwatfa, N. Darwish, G. Husseini, *Water* **2021**, *13*, 1327 DOI 10.3390/w13091327.
[69] W. Guo, H.-H. Ngo, J. Li, *Bioresour. Technol.* **2012**, *122*, 27.
[70] M. Hadidi, A. L. Zydney, *J. Membr. Sci.* **2014**, *452*, 97.
[71] I. Ielo, F. Giacobello, A. Castellano, S. Sfameni, G. Rando, M. R. Plutino, *Gels* **2022**, *8*, 26 DOI 10.3390/gels8010026.
[72] V. Costamagna, D. Wunderlin, M. Larrañaga, I. Mondragon, M. Strumia, *J. Appl. Polym. Sci.* **2006**, *102*, 2254.
[73] S. K. Lagergren, *Sven. Vetenskapsakad. Handingarl* **1898**, *24*, 1.
[74] W. J. Weber Jr, J. C. Morris, *J. Sanit. Eng. Div.* **1963**, *89*, 31.
[75] S. Roginsky, Y. B. Zeldovich, *Acta Phys. Chem. USSR* **1934**, *1*, 2019.
[76] I. Langmuir, *J. Am. Chem. Soc.* **1918**, *40*, 1361.
[77] H. M. F. Freundlich, *J. Phys. Chem.* **1906**, *57*, 1100.
[78] M. I. Temkin, *Acta physiochim. URSS* **1940**, *12*, 327.

Manuscript received: October 17, 2023
Revised manuscript received: December 7, 2023
Accepted manuscript online: December 28, 2023
Version of record online: ■■, ■■

RESEARCH ARTICLE

The development of functional blended polymeric beads based on the combination of polyethersulfone with a smart polymer P5-QPDMAEMA, combining the PDMAEMA responsiveness and the pillar[5]arenes host-guest properties, is shown. By post-functionalization subsequent synthetic steps, zwitterionic beads are produced and tested for dye pollutants absorption. These systems may open the way to the development of innovative composite materials for (waste)water treatment.

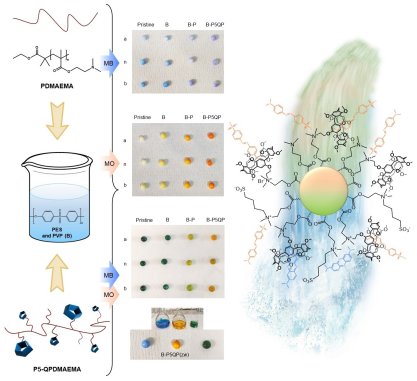

G. Rando, S. Sfameni, M. Milone, A. Mezzi, M. Brucale, A. Notti, M. R. Plutino**

1 – 17

Smart pillar[5]arene-based PDMAEMA/PES beads for selective dye pollutants removal: design, synthesis, chemical-physical characterization, and adsorption kinetic studies